Progress In Electromagnetics Research C, Vol. 94, 261–272, 2019

A Varactor-Tuned Aperture Coupled Dual Band Cylindrical Dielectric Resonator Antenna for C-Band Application

Arunodayam R. Anu[1, *], Parambil Abdulla[1], Puthenveetil M. Jasmine[2], and Thulaseedharan K. Rekha[1]

Abstract—A novel technique for designing a dual-band reconfigurable aperture coupled cylindrical dielectric resonator antenna is introduced here. The design is based on loading an aperture coupled cylindrical dielectric resonator antenna with a varactor diode located along the lines of the feed network. Loading the antenna with the varactor shifts the first and second resonant frequencies of the antenna. The resonant frequency can be continuously shifted from 4.75 GHz to 4.96 GHz in the lower band, and the resonant frequency of the higher band is shifted from 6.31 GHz to 6.40 GHz as the varactor diode bias voltage is increased from 1 V to 5 V. The proposed antenna offers a stable broadside radiation pattern at both bands and across the entire tunable frequency range for different bias voltages. The parametric analysis on the slot position is done to control the first and second resonant frequencies of the dual-band antenna. The proposed antenna plays a vital role in C-band (4 GHz–8 GHz) applications.

1. INTRODUCTION

In the latest communication technologies, high-performance antenna is regarded as one of the important devices to be used. In 1983, DRA started its expedition as a substitute to patch antennas. Though DRAs and microstrip patch antennas have their own merit and potential, DRAs appear to be a possible replacement for the microstrip patch antenna, especially at millimeter-wave frequencies. A number of DRAs have been used because of their advantages such as small size, high radiation efficiency, ease of excitation, and low-temperature coefficient. There are many reconfigurable microstrip patch antennas [1–8], but only a few reconfigurable DRAs have been reported in the literature. So more attention has been paid to frequency adjustable DRAs such as using multiple parasitic strips [9], shifting the spiral position along the DRA surface [10], and loading cap [11]. Frequency tunable designs using a parasitic slot have been studied theoretically and experimentally [12], but they are used for the design stage rather than post manufacturing tuning. Tunable DRAs using varactor diode [13], pin diodes [14], water [15], and colloidal dispersion [16] have been proposed which are also complicated.

This article presents tuning of the operating frequency of an aperture coupled cylindrical dielectric resonator antenna (CDRA) by using a varactor diode. The aperture-coupled source is mostly used for DRAs because of its possibility of combination with monolithic microwave integrated circuits (MMICs). The varactor is used as a load to alter the resonant frequency of the antenna. Varactor diode has better switching speed, reliability and lowers applied voltage. It offers a capacitance that can be continually tuned by varying the diode bias voltage. Hence the effective electric length changes leading to the shift of antenna resonance to the higher frequencies.

Received 23 May 2019, Accepted 26 July 2019, Scheduled 5 August 2019
* Corresponding author: Arunodayam R. Anu (aranu17@gmail.com).
[1] School of Engineering, Cochin University of Science and Technology, Cochin, Kerala, India. [2] M.E.S. College Marampally, Aluva, Kerala, India.

2. THEORY

DRAs are of different shapes like rectangle, cylinder, hemisphere, etc. One of the important parameters needed to design the dielectric resonator antenna (DRA) is resonant frequency. The resonant frequency of a DRA depends on its operating mode, dielectric constant, and physical shape. Simple analysis for the cylindrical DRA was carried out in [17] using a magnetic wall model. In the analysis, an approximate solution for the fields inside a cylinder was obtained by assuming that the surfaces were perfect magnetic conductors, with the feed probe temporarily ignored. For such a cavity, wave functions transverse electric (TE) and transverse magnetic (TM) modes to z are given as

$$\psi_{TE_{npm}} = J_n\left(\frac{X_{np}}{a}\rho\right)\left\{\begin{array}{c}\sin n\phi\\ \cos n\phi\end{array}\right\}\sin\left[\frac{(2m+1)\,\pi z}{2d}\right] \tag{1}$$

$$\psi_{TM_{npm}} = J_n\left(\frac{X'_{np}}{a}\rho\right)\left\{\begin{array}{c}\sin n\phi\\ \cos n\phi\end{array}\right\}\cos\left[\frac{(2m+1)\,\pi z}{2d}\right] \tag{2}$$

where J_n is the Bessel function of the first kind,

$$J_n\left(X_{np}\right) = 0, \quad J'_n\left(X'_{np}\right) = 0 \tag{3}$$

$n = 1, 2, 3 \ldots$, $p = 1, 2, 3 \ldots$, $m = 0, 1, 2, \ldots$. The separation equation $k_p^2 + k_z^2 = k^2 = \omega^2\mu\varepsilon$ leads to an expression for the resonant frequency of npm mode.

$$f_{npm} = \frac{1}{2\pi a\sqrt{\mu\varepsilon}}\sqrt{\left\{\frac{X_{np}^2}{X_{np}'^2}\right\} + \left[\frac{\pi a}{2d}\,(2m+1)\right]^2} \tag{4}$$

The dominant mode is the one which has the lowest resonant frequency. This occurs for $m = 0$, $n = 1$, $p = 1$, where $X'_{11} = 1.841$. In the case of cylindrical DRA, TM_{110} mode has the lowest resonant frequency given by

$$f_{dom} = \frac{1}{2\pi a\sqrt{\mu\varepsilon}}\sqrt{\left\{X_{11}'^2\right\} + \left[\frac{\pi a}{2d}\right]^2} \tag{5}$$

The theoretical value of the resonant frequency of the proposed antenna computed using Equation (5) is 6.29 GHz.

3. ANTENNA CONFIGURATION

The geometry of the proposed reconfigurable CDRA together with the varactor diode biasing circuit is presented in Figure 1. The CDRA consists of a dielectric resonator made of alumina material (Al_2O_3) having a permittivity of $\varepsilon_r = 9.8$. It has a radius 7.0 mm and height 5.0 mm located at an offset position of 1 mm in the negative X-direction and 2.5 mm along positive Y-direction in the ground plane of an FR4 substrate with a thickness of 1.6 mm, length 80 mm, and width 70 mm. The CDRA is excited by a rectangular slot etched on the ground plane. The rectangular slot having width 0.25 mm and length 8 mm is located at position (−1.8 mm, −0.5 mm, 1.6 mm). The feed line, composed of a 50 Ω input impedance microstrip line and a stub line (at position −4.3 mm, 1.5 mm, 0 mm), is etched on the other side of the substrate. The microstrip line has length 35 mm and width 3 mm, and the stub line has length 9.3 mm and width 3 mm. A varactor diode is placed in between the microstrip line and stub line in order to tune the resonant frequency.

Figure 2(a) and Figure 2(b) represent the top and bottom views of the antenna prototype. In Figure 2(b), the varactor diode BB857 biased with a reverse voltage supplied through two dc bias lines connected across a 9 V battery is shown. The details of the varactor are listed in Table 1. The dc bias lines are connected to the feed network at the bottom part of the substrate containing varactor diode, RF choke inductors, and input voltage.

Figure 3 shows typical capacitance of a BB857 varactor (from Infineon) as a function of its bias voltage. As the bias voltage changes from 1 V to 28 V, the varactor capacitance varies from 6.6 pF to 0.45 pF.

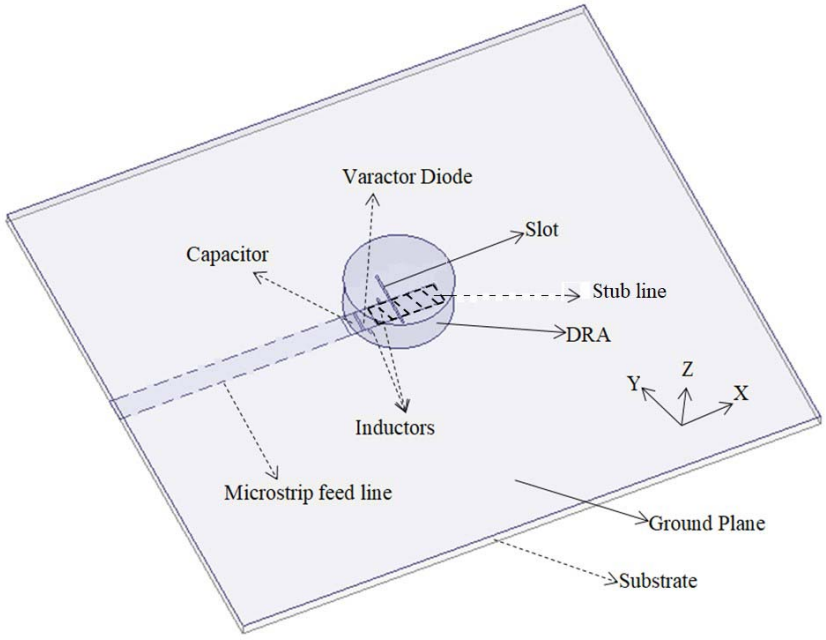

Figure 1. The configuration of the proposed cylindrical dielectric resonator antenna.

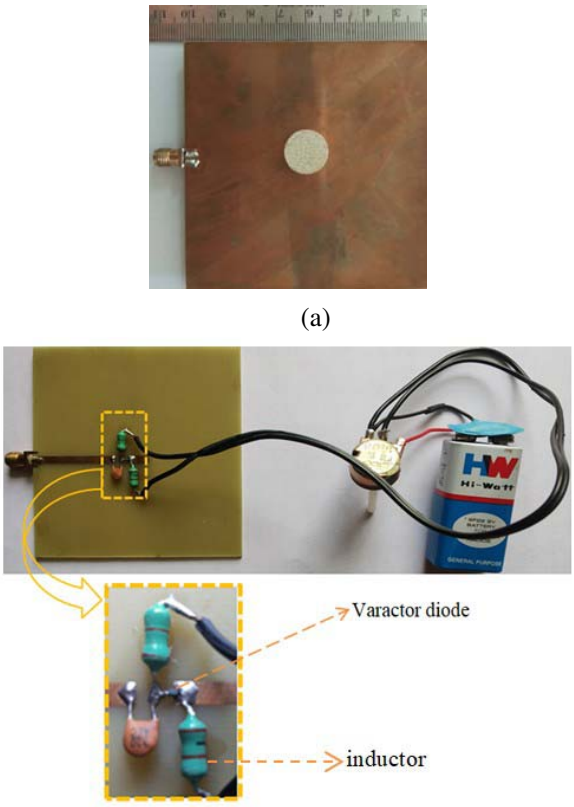

Figure 2. (a) Top view of antenna prototype. (b) Bottom view of antenna prototype.

Table 1. Varactor details.

Type Number	BB857
Package	SC-79
Version	SOD323
Manufacturer	Infineon
Reverse Voltage	30 V
Diode series resistance	1.5 Ω
Diode Capacitance	0.45–6.6 pF

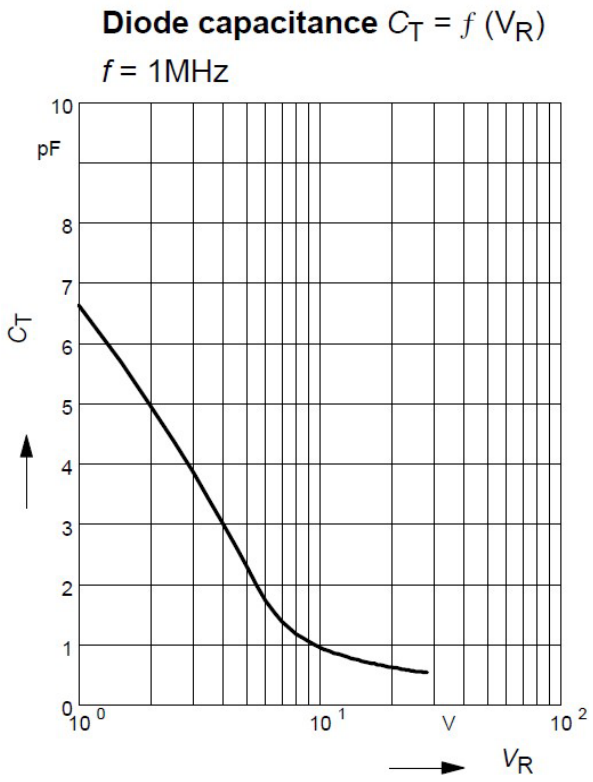

Figure 3. The typical capacitance of a BB857 varactor (from Infineon) as a function of its bias voltage.

4. ANALYSES OF KEY PARAMETERS

The first step to design the proposed dual-band reconfigurable antenna is to analyze the effect of slot coupled CDRA**.** The second step involves the combination of varactor diode and slot coupled CDRA, and the final step is the adjustment of the slot position in order to obtain the proposed reconfigurable dual-band antenna.

4.1. Slot Coupled CDRA

The antenna consists of an FR4 substrate with a thickness of 1.6 mm, length 80 mm, and width 70 mm used as the ground plane. A rectangular slot having width 0.25 mm and length 8 mm is located at position (−1.8 mm, −0.5 mm, 1.6 mm). The feed line composed of a 50 Ω input impedance microstrip line having length 45 mm and width 3 mm is etched on the other side of the substrate. Antenna with

slot alone was considered before placing the CDRA above the slot. The slot resonance without the CDRA is obtained at 11.15 GHz. The reflection characteristics are studied by placing the CDRA above the slot. The CDRA consists of a dielectric resonator made of alumina material (Al_2O_3) having a permittivity of $\varepsilon_r = 9.8$. It has a radius 7 mm and height 5 mm located at an offset position of 1 mm in the negative X-direction and 2.5 mm along positive Y-direction in the ground plane. The rectangular slot etched on the ground plane of the dielectric substrate is used to excite the CDRA. The CDRA and slot together yield a dual resonance antenna with good radiation characteristics. The effects of the CDRA and slot are coupled together, and any minor change in either structure parameter also affects the other resonance. The CDRA placed above the slot increases the effective permittivity of the slot that further shifts the slot resonance downwards. As the two resonant structures are combined, dual resonances at 6.2 GHz and 8.29 GHz are obtained as shown in Figure 4.

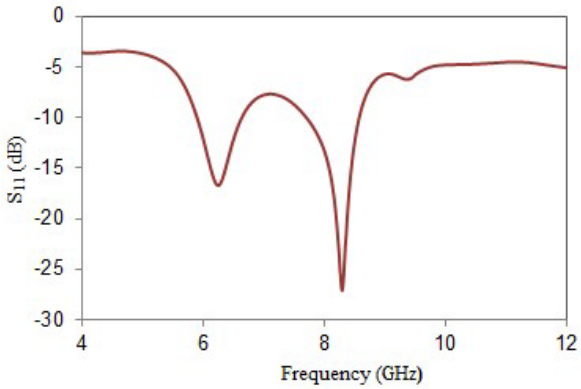

Figure 4. Simulated S_{11} of the slot with CDRA.

4.2. Varactor Tuned Slot Coupled Dual-Band CDRA

A varactor diode is placed in between the microstrip line and stub line in order to tune the resonant frequency. The microstrip line has length 35 mm and width 3.0 mm, and the stub line has length 9.3 mm and width 3.0 mm. With combining the circuit with a varactor diode, biasing circuit and fixing the slot position at 2.7 mm in the negative X-direction, dual bands are developed. The biasing circuit consists of two RF choke inductors of 100 mH and a dc block capacitor of 100 pF. The dc block capacitor is chosen to isolate the RF components from the dc signal and the RF choke inductor isolate the RF signal from the dc signal. With changing the varactor biasing, the dual bands can be tuned as shown in Figure 5. To simulate the change in varactor capacitance, dc block capacitance, and inductance values in Ansoft HFSS [18], a lumped RLC boundary condition is applied to the corresponding regions.

Table 2 shows the first and second resonance values of the simulated S_{11} for the capacitance values from 4.08 pF to 4.16 pF at slot position 2.7 mm in the negative X direction.

By changing the position of the slot at 2.6 mm along the negative X-direction and keeping all other

Table 2. Simulated resonance values of S_{11} at slot position 2.7 mm in negative X direction.

Capacitance (pF)	**Simulated Values**	
	1st resonance	2nd resonance
4.08	6.11 GHz	6.39 GHz
4.10	6.12 GHz	6.40 GHz
4.12	6.13 GHz	6.41 GHz
4.14	6.14 GHz	6.42 GHz
4.16	6.15 GHz	6.43 GHz

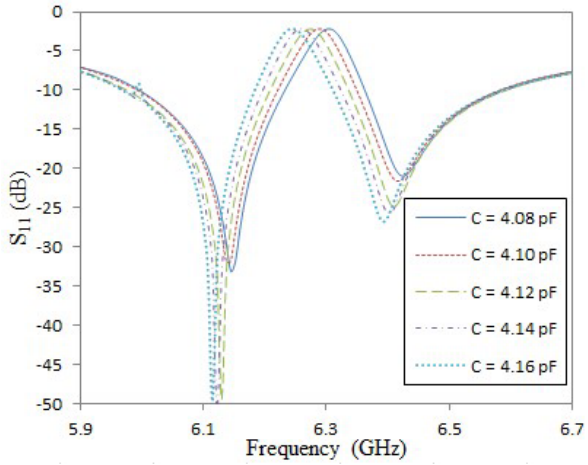

Figure 5. Simulated S_{11} of the slot at position 2.7 mm in the negative X direction for different varactor capacitance.

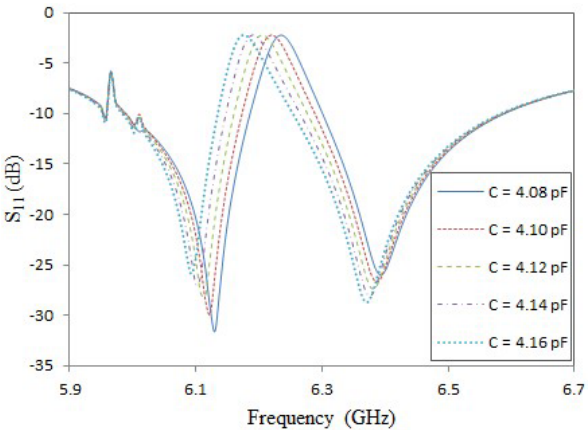

Figure 6. Simulated S_{11} of the slot at position 2.6 mm in the negative X direction for different varactor capacitance.

parameters same, dual resonances are obtained, and with changing the same varactor capacitance from 4.08 pF to 4.16 pF a reconfigurable dual-band antenna is obtained as shown in Figure 6. However, there is a shift in the resonance frequency at both bands as the slot position is changed from 2.7 mm to 2.6 mm in the negative X direction.

Table 3 shows the first and second resonance values of the simulated S_{11} for capacitance values from 4.08 pF to 4.16 pF at slot position 2.6 mm in the negative X direction.

By changing the position of the slot at 2 mm along the negative X-direction and keeping all other parameters same, dual resonances are obtained as depicted in Figure 7. Here the higher band resonance shows negligible change, and the lower resonance frequency is tuned by changing the varactor capacitance from 4.08 pF to 4.16 pF.

Table 4 shows the first and second resonance values of the simulated S_{11} for varactor capacitance values from 4.08 pF to 4.16 pF at slot position 2 mm in the negative X direction.

Similarly, by changing the position of the slot at 1.8 mm along the negative X-direction and keeping all other parameters same, dual resonances are obtained. Here there is also a negligible change in the higher band. The simulated S_{11} for capacitance values corresponding to the voltage 1 V to 5 V in the datasheet of the varactor is shown in Figure 8.

Table 5 shows the first and second resonance values of the simulated S_{11} for voltage values of 1 V to 5 V at slot position 1.8 mm in the negative X direction.

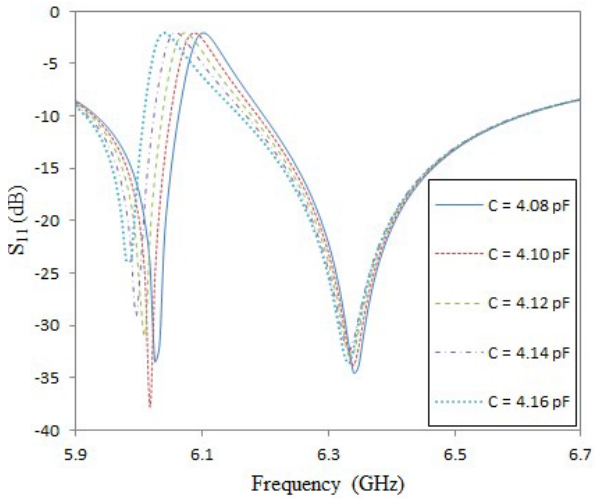

Figure 7. Simulated S_{11} of the slot at position 2 mm in the negative X direction for different varactor capacitance.

Table 3. Simulated resonance values of S_{11} at slot position 2.6 mm in negative X direction.

Capacitance (pF)	**Simulated Values**	
	1st resonance	2nd resonance
4.08	6.09 GHz	6.37 GHz
4.10	6.10 GHz	6.377 GHz
4.12	6.11 GHz	6.385 GHz
4.14	6.12 GHz	6.3925 GHz
4.16	6.13 GHz	6.4 GHz

Table 4. Simulated resonance values of S_{11} at slot position 2 mm in negative X direction.

Capacitance (pF)	**Simulated Values**	
	1st resonance	2nd resonance
4.08	5.98 GHz	6.335 GHz
4.10	5.995 GHz	6.335 GHz
4.12	6.01 GHz	6.34 GHz
4.14	6.0175GHz	6.34 GHz
4.16	6.025 GHz	6.34 GHz

Table 5. Simulated resonance values of S_{11} at slot position 1.8 mm in negative X direction.

Voltages	**Simulated Values**	
	1st resonance	2nd resonance
1 V	4.75 GHz	6.205 GHz
2 V	4.825 GHz	6.235 GHz
3 V	5.155 GHz	6.25 GHz
4 V	5.23 GHz	6.19 GHz
5 V	5.275 GHz	6.25 GHz

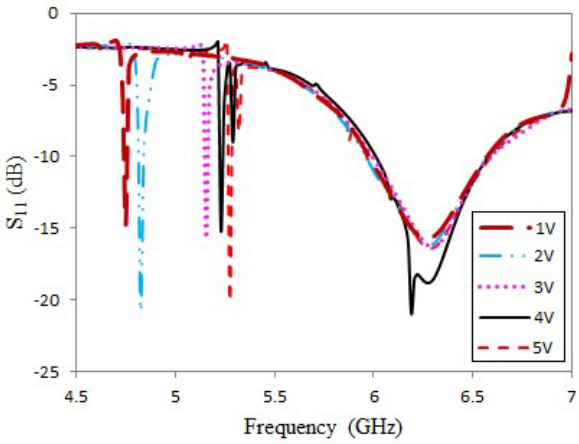

Figure 8. Simulated S_{11} of the slot at position 1.8 mm in the negative X direction for voltage values of 1 V to 5 V.

5. RESULTS AND DISCUSSION

A frequency tunable varactor controlled CDRA is simulated using Ansoft HFSS software. The input reflection coefficient is measured by Rohde & Schwarz ZVL 13 Vector Network Analyzer. To achieve robust coupling, a magnetic current source (an aperture) is placed in a range of high magnetic field. The DRA centered above the slot ensures robust coupling to inner magnetic fields. The slot width also shows a major role in guiding the amount of power coupled to DRA. The fundamental TM_{110} mode of the CDRA is excited. To attain a frequency-tunable antenna, the varactor diode should be placed in locations where the current paths can be affected. The electrical lengths of some of the current paths can become longer which causes the antenna to resonate at lower frequencies. The electrical path lengths are affected which in turn changes the resonant frequencies of the antenna. The simulated surface current distributions of reconfigurable aperture coupled CDRA at resonant frequencies 4.75 GHz and 5.155 GHz are depicted in Figures 9(a)–9(b). Each diagram shows a different surface current distribution. As the voltage is changed, the surface current distribution is also changed. The change in the surface current distribution results in a tunable resonance antenna. In Figure 9(a), the surface current distribution at 1 V is given, which shows that at the first resonance, the electric current is denser around the slot than the first resonance at 3 V, as a result of the resonant frequency shifts to a higher frequency.

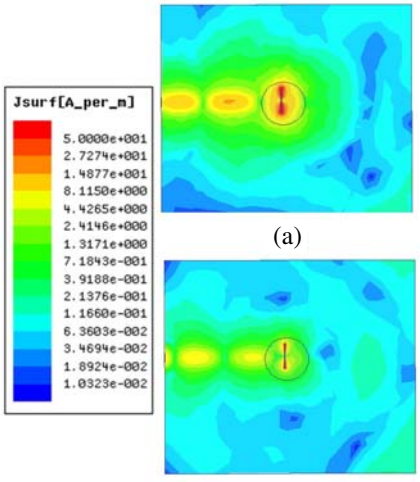

Figure 9. Surface current distribution at the first resonance (a) 1 V, (b) 3 V.

Table 5 shows the shift in simulated resonant frequency of the antenna from lower frequency 4.75 GHz to a higher frequency of 5.275 GHz in the lower band and small changes between 6.205 GHz and 6.25 GHz in the higher band as the voltage is increased from 1 V to 5 V. Figure 10 shows the measured lower band reflection coefficient of the proposed antenna at different reverse bias voltages. The measured resonant frequency of the antenna is shifted from 4.75 GHz to 4.96 GHz in the lower band. The lower band has a constant bandwidth of 8% (4.66 GHz–5.08 GHz for 1 V).

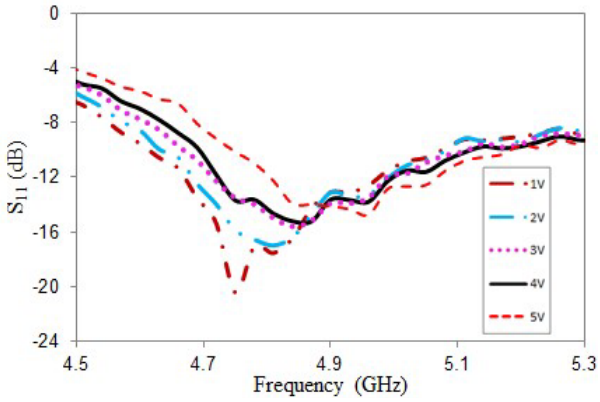

Figure 10. Measured S_{11} of the lower band of the proposed antenna.

Figure 11 shows the measured lower and upper band reflection coefficients of the proposed antenna at different reverse bias voltages from 1 V to 5 V. The resonant frequency of the higher band shows small changes between 6.31 GHz and 6.40 GHz and has a bandwidth of 21% (5.68 GHz–7.06 GHz for 1 V).

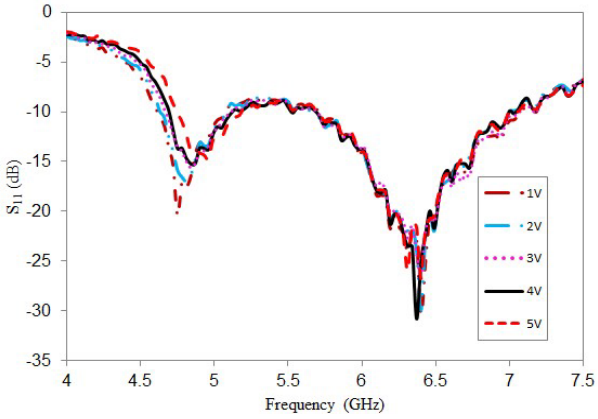

Figure 11. Measured S_{11} of the proposed antenna.

Table 6 shows the first and second resonance values of the measured S_{11} for voltage values of 1 V to 5 V at slot position 1.8 mm in the negative X direction.

Figure 12 shows the simulated and measured radiation patterns of the proposed antenna for the operating frequencies 4.75 GHz, 6.3 GHz, and 5.155 GHz for three different voltages of 1 V, 2 V, and 3 V, respectively. Symmetrical broadside radiation patterns are obtained in both the planes.

Figure 13 shows the simulated and measured gains of the antenna. The simulated gain has a peak value of 6.38 dBi, and measured gain has a peak value of 7.23 dBi at the lowest resonant frequency band. The simulated gain has a peak gain of 7.24 dBi and measured the gain of 5.74 dBi at the highest resonant frequency band.

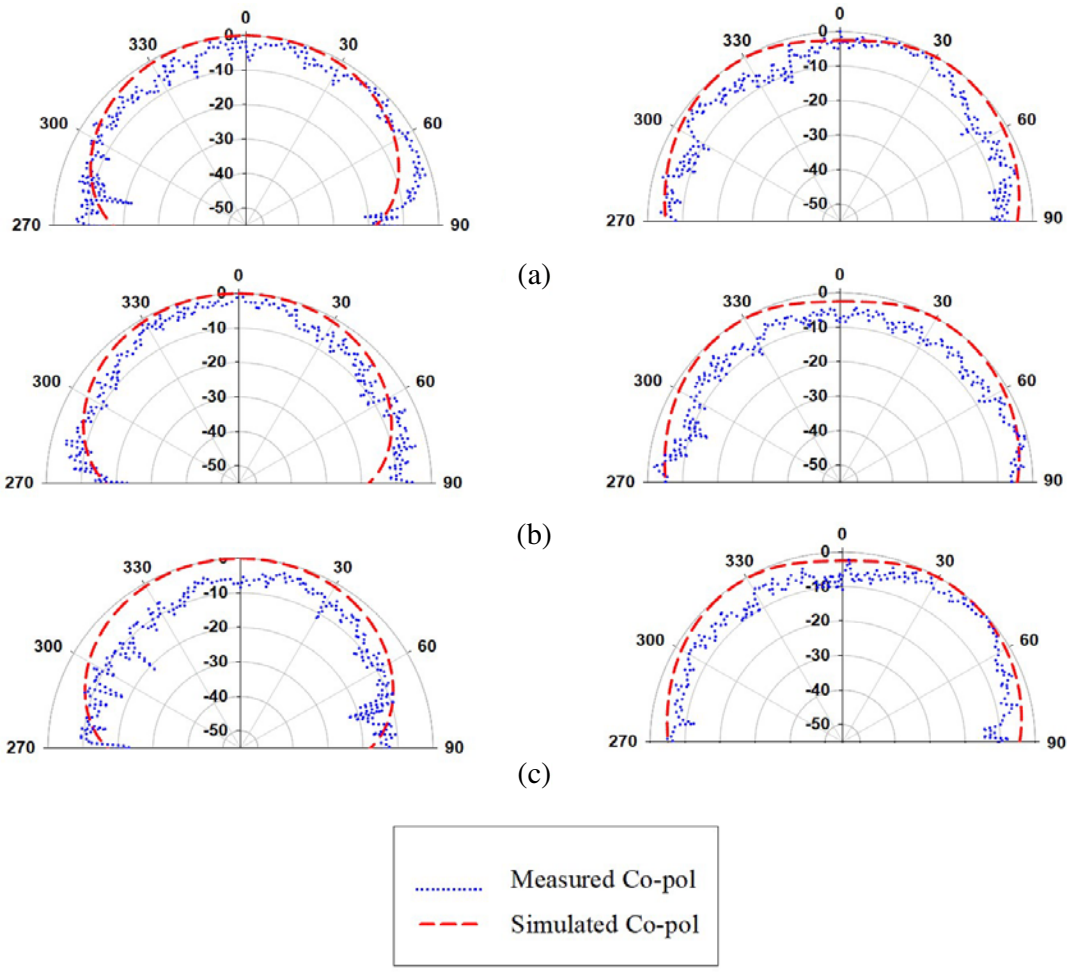

Figure 12. Simulated and measured E and H plane co-polarization radiation patterns of the proposed antenna at (a) 1 V, 4.75 GHz, (b) 2 V, 6.3 GHz, (c) 3 V, 5.155 GHz.

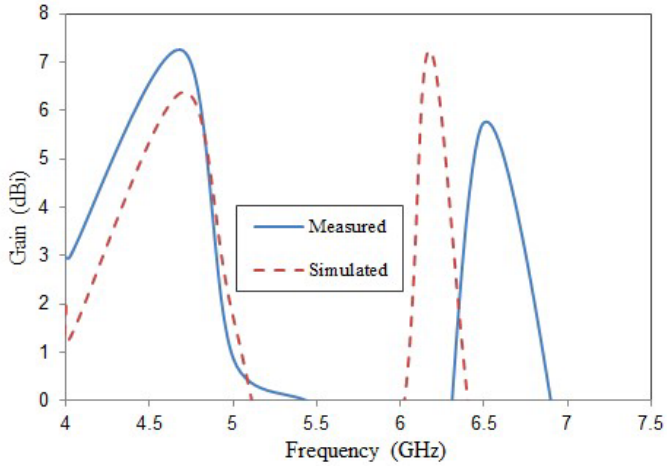

Figure 13. Measured and Simulated gain of the proposed antenna.

Table 6. Measured resonance values of S_{11} at slot position 1.8 mm in negative X direction.

Voltages	Measured Values	
	1st resonance	2nd resonance
1 V	4.75 GHz	6.31 GHz
2 V	4.81 GHz	6.34 GHz
3 V	4.84 GHz	6.37 GHz
4 V	4.87 GHz	6.40 GHz
5 V	4.96 GHz	6.40 GHz

6. CONCLUSION

This work shows a varactor controlled rectangular slot coupled frequency reconfigurable cylindrical dielectric resonator antenna. The bias voltage applied to the varactor loaded CDRA can provide a dynamic frequency tuning. The resonant frequency of the antenna can be tuned from 4.75 GHz to 4.96 GHz in the lower band (having a 10 dB impedance bandwidth of 8%), and the upper band changes from 6.31 GHz to 6.40 GHz (having a 10 dB impedance bandwidth of 21%) as the varactor diode capacitance is increased from 1 V to 5 V. The shift in the dual resonance tuning and tuning of both lower resonance and higher resonance is obtained by changing the slot position. The application of the proposed antenna includes a wide range of applications in C-band such as satellite communication systems, weather radar systems, Wi-Fi, and ISM band applications. The C-band is known to perform better for satellite communication in adverse weather condition.

ACKNOWLEDGMENT

The authors would like to acknowledge the financial assistance and infrastructural support from the University Grants Commission, Government of India.

REFERENCES

1. Majid, H. A., M. K. A. Rahim, M. R. Hamid, and M. F. Ismail, "Frequency reconfigurable microstrip patch slot antenna with directional radiation pattern," *Progress In Electromagnetics Research Letters*, Vol. 144, 319–328, 2014.
2. Alkanhal, M. A. and A. F. Sheta, "A novel dual-band reconfigurable square – Ring microstrip antenna," *Progress In Electromagnetics Research Letters*, Vol. 70, 337–349, 2007.
3. Saed, M. A., "Reconfigurable broadband microstrip antenna fed by a coplanar waveguide," *Progress In Electromagnetics Research Letters*, Vol. 55, 227–239, 2005.
4. Shynu, S. V., G. Augustin, C. K. Aanandan, P Mohanan, and K. Vasudevan, "Design of compact reconfigurable dual-frequency microstrip antennas using varactor diodes," *Progress In Electromagnetics Research Letters*, Vol. 60, 197–205, 2006.
5. Simons, R. N., D. Chun, and L. P. B. Katehi, "Microelectromechanical systems (MEMS) actuators for antenna reconfigurability," *IEEE MTT-S Int. Microwave SymDigest*, 215–218, May 2001.
6. Simons, R. N., D. Chun, and L. P. B. Katehi, "Polarization reconfigurable patch antenna using Microelectromechanical Systems (MEMS) actuators," *IEEE AP-S Sym. Digest*, 6–9, June 2002.
7. Chiao, J. C., S.-Y. Cheng, J. L. Chang, I. M. Chio, Y. Kang, and J. Hayasaka, "MEMS reconfigurable antennas," *Int. J. RF Microwave CAE*, Vol. 11, 301–309, 2001.
8. Zhu, H. L., X. H. Liu, S. W. Cheung, and T. I. Yuk, "Frequency-reconfigurable antenna using metasurface," *IEEE Transactions on Antennas and Propagation*, Vol. 62, No. 1, 80–85, 2014.

9. Ng, H. K. and K. W. Leung, " Frequency tuning of the linearly and circularly polarized dielectric resonator antennas using multiple parasitic strips," *IEEE Transactions on Antennas and Propagation*, Vol. 54, No. 1, 225–230, 2006.
10. Sulaiman, M. I. and S. K. Khamas, " Frequency tuning of a singly fed rectangular dielectric resonator antenna with a wideband circular polarization," *IEEE Loughborough Antennas Propagat. Conf.*, Vol. 53, No. 3, 1229–1232, 2005.
11. Ng, H. K. and K. W. Leung, "Frequency tuning of the dielectric resonator antenna using a loading cap," *IEEE Trans. Antennas Propagat.*, Vol. 53, No. 3, 1229–1232, 2005.
12. Leung, K. W. and K. K. So, " Frequency tunable designs of the linearly and circularly polarized dielectric resonator antenna using a parasitic slot," *IEEE Transactions on Antennas and Propagation*, Vol. 53, No. 1, 572–576, 2005.
13. Hao, C. X., B. Li, K. W. Leung, and X. Q. Sheng, "Frequency-tunable differentially fed rectangular dielectric resonator antennas," *IEEE Antennas and Wireless Propagation Letters*, Vol. 10, 2011.
14. Desjardins, D., A. McNamara, S. Thirakouna, and A. Petosa "Electronically frequency-reconfigurable rectangular dielectric resonator antennas," *IEEE Transactions on Antennas and Propagation*, Vol. 60, No. 6, 2997–3002, June 2012.
15. O'Keefe, S. G. and S. P. Kingsley, "Tunability of liquid dielectric resonator antennas," *IEEE Antennas Wireless Propag. Lett.*, Vol. 6, 533–536, 2007.
16. Huff, G. H., D. L. Rolando, P. Walters, and J. McDonald, "A frequency reconfigurable dielectric resonator antenna using colloidal dispersions," *IEEE Antennas Wireless Propag. Lett.*, Vol. 9, 288–290, 2010.
17. Long, S. A., M. W. McAllister, and L. C. Shen, "The resonant cylindrical dielectric cavity antenna," *IEEE Transactions on Antennas and Propagation*, Vol. 31, 406–412, May 1983.
18. Ansoft High Frequency Structure Simulator (HFSS), version 15, Ansoft Corporation, Pittsburgh, U.S.A.